# Electronic States of $Cr(CO)_5$

P. Jeffrey Hay

*Contribution from the Theoretical Division, Los Alamos Scientific Laboratory,
University of California, Los Alamos, New Mexico 87545. Received August 26, 1977*

Abstract: The electronic states of $Cr(CO)_5$ are investigated using ab initio SCF and configuration interaction (CI) wave functions in a small Gaussian basis. Using fixed bond lengths the $^1A_1$ state of the C_{4v} square pyramid is found to be the lowest electronic state. The $^3A_2'$ state of the D_{3h} trigonal bipyramid is found to lie 9 kcal/mol higher in energy. The inclusion of electron correlation effects appears to play an important role in the relative ordering of states. Sixteen electronic states are investigated at various geometries, and the visible absorption band (500 nm) is attributed to the $^1A_1 \rightarrow {}^1E$ transition of the C_{4v} form of $Cr(CO)_5$.

I. Introduction

The $Cr(CO)_5$ molecule, which can be generated photolytically from $Cr(CO)_6$ or its derivatives,

$$Cr(CO)_6 \xrightarrow{h\nu} Cr(CO)_5 + CO$$

$$Cr(CO)_5X \xrightarrow{h\nu} Cr(CO)_5 + X$$

$$\xrightarrow{h\nu} Cr(CO)_4X + CO$$
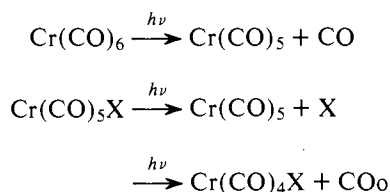
plays a central role in the photochemistry of $Cr(CO)_6$.[1,2] Alternatively it can be prepared by cocondensation of Cr atoms with CO in a matrix environment. It also serves as a prototype for the heavier d^6 species $Mo(CO)_5$ and $W(CO)_5$ with related photochemistry. Since this "coordinatively unsaturated" species with 16 valence electrons surrounding the metal is 2 electrons short of attaining the stable 18-electron configuration, it is quite reactive. Recently several experimental studies have sought to characterize the geometry and electronic structure using matrix isolation techniques. Ozin and co-workers,[3,4] cocondensing metal atoms and CO, analyzed the infrared spectrum of $Cr(CO)_5$ using various isotopic combinations. Photolyzing the hexacarbonyl in inert matrices, Turner et al.[5-8] have also studied the infrared spectrum and observed a visible (18 000 cm^{-1}) and UV (44 000 cm^{-1}) absorption band. The former studies yielded an interpretation of a trigonal bipyramid (TBP) structure (**1**) having D_{3h} symmetry[3] while the latter studies showed a square pyramid (SP) structure (**2**) with C_{4v} symmetry.[8] In the studies by Ozin,

heating of the matrix to 40–45 K converted the TBP form into a SP form.[4] Analysis of all these results has led to the interpretation[4,7b,9] that the latter may be the thermodynamically more stable form. Other $M(CO)_5$ species which have been characterized include the closed-shell d^8 $Fe(CO)_5$ molecule[10] with a TBP geometry, the d^7 $Mn(CO)_5$ radical[11] which appears to have a SP geometry, and the d^5 $V(CO)_5$ species[12] with a TBP geometry.

Simple theoretical considerations lead one to anticipate a singlet d^6 ground state $[(e)^4(b_2)^2, {}^1A_1]$ for the SP and a triplet ground state $[(e'')^4(e')^2, {}^3A_2']$ for the TBP. The triplet state correlates with the ^3E state of the SP $[(e)^3(b_2)^2(a_1)^1]$. Semiempirical calculations,[13,14] including extended Hückel calculations, have been carried out on $M(CO)_5$ species which predict that the $^1A_1$ state of $Cr(CO)_5$ prefers the SP geometry with a $(CO)_{ax}$–Cr–$(CO)_{eq}$ bond angle of $\sim 90°$. Such calcu-

lations are not capable, however, of providing accurate information concerning the relative energies of electronic states having different spin multiplicities and different geometries. In addition, since the matrix isolation experiments show a pronounced effect on the absorption spectrum by the matrix, it is possible that the structure of the molecule in the matrix could differ in the gas phase.

Consequently, an ab initio investigation of the low-lying electronic states of the $Cr(CO)_5$ molecule was undertaken. The calculations of the relative energies of states at several different geometries should give information concerning the electronic ground state, the molecular geometry, and the absorption spectrum. We present here both self-consistent field (SCF) single-configuration calculations as well as results from configuration interaction (CI) calculations involving several hundred configurations. The inclusion of electron correlation effects by the CI calculations appears to play a major role in determining the relative energies of states, in contrast to compounds of first- and second-row atoms where a single configuration SCF wave function is often sufficient to predict the geometry and relative ordering of the lowest states. Recently SCF calculations on the SP $^1A_1$ and TBP $^3A_2'$ states have been reported using a more extensive basis by Demuynck, Strich, and Veillard.[15] These will form a useful basis for comparison with the present calculations, which use a much smaller basis, but which also include CI results. In fact this is one of the few attempts to date to investigate the effect of electron correlation effects in transition metal complexes.[26] An alternative to the approach pursued here is the implicit inclusion of atomic correlation effects into an effective potential, which also serves to replace the inner core orbitals.[27] Nonetheless the current results should be interpreted quite cautiously in light of the basis set restrictions and the lack of geometry optimization until more experience in the area of metal complexes has been gained.

II. Details of the Calculation

A. Basis Sets and Geometries. A minimal basis set (1s, 2s, 2p) of contracted Gaussian functions (STO-3G)[16] was used on the C and O atoms. For Cr the (12s, 8p, 4d) basis of Roos, Vinot, and Veillard[17] was augmented by two primitive p functions to represent the 4p orbital and an additional 3d function with exponent 0.0972. This set was contracted to 1s, 2s, 3s, 4s, 2p, 3p, 4p, 3d, 3d', and 3d'' using the general contraction scheme of Raffenetti,[18] and molecular integrals involving the resulting 81 basis functions were computed using Raffenetti's BIGGMOLI integral program. Even without the additional 3d'' basis function, this basis would be of comparable accuracy to the one used by Hillier and Saunders[19] in their earlier study of $Cr(CO)_6$.

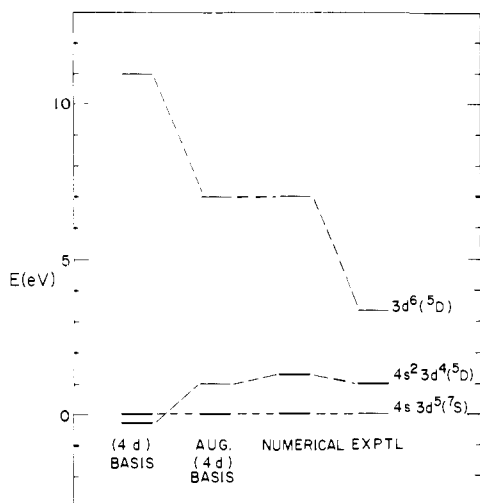The need for an additional 3d function and for a flexible 3d

Figure 1. Electronic states of the Cr Atom. Results of Hartree–Fock basis set calculations are compared with numerical calculations and with experiment.

Table I. Atomic Excitation Energies (eV) for the Cr Atom

	SCF calcns			CI	
Excitation	(4d)	Aug (4d)	Numer	Calcns	Expt
$4s^23d^4(^5D) \leftarrow 4s3d^5(^7S)$	−0.22	0.99	1.27		1.00
$3d^6(^5D) \leftarrow 4s3d^5(^7S)$	11.25	6.97	7.02		4.40
$3d^6(^5D) \leftarrow 4s^23d^4(^5D)$	11.03	5.98	5.75	4.09	3.40

basis set has been discussed by the author[20] and will be summarized here. The $Cr(CO)_5$ molecule may possess a $(3d)^6$ configuration as in the parent molecule $Cr(CO)_6$ as well as configurations such as $(3d)^5(4s)^1$. In order to describe these configurations consistently in the molecule the states of the atom itself should also be properly represented.

The use of a standard basis set such as the (4d) basis of Roos et al. which has been optimized for the $(3d)^4(4s)^2$ configuration can lead to large errors in the relative position of the $(3d)^6$ ^5D state. As shown in Figure 1, Hartree–Fock calculations in the (4d) basis place the $3d^6$ state 11 eV above the ground state compared to 7 eV from exact numerical HF results. The "augmented (4d)" basis (see also Table I) gives results in excellent agreement with the numerical HF calculations. Roos et al. also recommended the addition of a diffuse function but for the different reason of providing a better metal–ligand overlap.

A discrepancy of over 3 eV still persists between SCF calculations and experimental term values. This can only be attributed to electron correlation effects and these shall be treated here by configuration interaction (CI) techniques. By including all single and double excitations relative to the 3d and 4s orbitals in Cr atom, this final discrepancy can be reduced to about 0.5 eV (Table I).

All calculations were performed with fixed bond lengths where the Cr–C (1.916 Å) and C–O (1.171 Å) distances were taken[21] from $Cr(CO)_6$. The geometric distortions involved bending of two equatorial CO moieties about the central Cr.

The bending angle θ, defined above, has the values 90 (C_{4v} symmetry, SP), 105, 120 (D_{3h} symmetry, TBP), and 135°. All C–O linkages were held linear.

B. SCF and CI Calculations. Self-consistent field calculations were performed for the $^3B_2[(3a_2)^2(11b_1)^2(23a_1)^1(11b_2)^1]$ state at the previously described geometries using the spin-restricted open-shell Hartree–Fock procedure. For the SP structure, calculations were also carried out on the $^1A_1$-$[(3a)_2)^2(11b_1)^2(11b_2)^2]$ closed-shell state. These orbitals then formed the starting point for carrying out configuration interaction (CI) calculations which are needed for examining several excited states of a given symmetry and for incorporating the electron correlation effects discussed above. The CI calculations based on $^1A_1$ orbitals used improved virtual orbitals[22] obtained by removal of the $3a_2$ orbital, while the CI calculations based on $^3B_2$ orbitals used virtuals obtained by averaging the field formed by removal of the $23a_1$ or $11b_2$ orbitals. The innermost 29 orbitals were always held doubly occupied and the lowest 12 virtual orbitals were retained. In addition the five components of a 3d-like orbital for correlating the 3d shell were added from MCSCF atomic calculations and orthogonalized for the others, yielding a total of 36 occupied and virtual orbitals in the CI calculations.

All states arising from the 3d manifold (the $23a_1$, $3a_2$, $11b_1$, and $11b_2$ orbitals) were constructed. In C_{2v} symmetry this resulted in four $^1A_1$ states and two states each of $^{1,3}A_2$, $^{1,3}B_1$, and $^{1,3}B_2$ symmetry, or 16 states in all. These states formed the zero-order reference configurations $\{\psi_0\}$ for the CI calculations. All single and double excitations out of the four highest orbitals in $\{\psi_0\}$ were constructed to account for correlation and relaxation effects in the 3d shell, and single excitations relative to the remaining orbitals were included to allow for readjustments due to the use of ground-state orbitals. All these configurations were then screened using perturbation theory and all those contributing at least 5×10^{-5} au to any root were retained in the final CI calculation. The numbers of spin configurations before and after (at $\theta = 90°$) were as follows: $^1A_1$ (1506–664), $^1A_2$ (1496–622), $^1B_1$ (1494–633), $^1B_2$ (1494–594), $^3A_2$ (2193–925), $^3B_1$ (2191–923), $^3B_2$ (2191–867). Very little difference was found between using $^1A_1$ and $^3B_2$ orbitals for the SP geometry.

To investigate higher states such as metal to ligand charge transfer excitations, a much simpler CI scheme which included only single excitations relative to the Hartree–Fock $^1A_1$ state was followed. A more sophisticated treatment did not appear to be warranted because of the limitations of the basis set in describing these higher states not involving solely 3d orbitals.

Representative computer times (CDC 7600 total elapsed time) were as follows: integral evaluation using BIGGMOLI, 40 min; open-shell SCF calculations, 2.5 min/iteration (usually requiring 20–40 iterations); integral transformation, 17 min; CI calculations, 1–2 min for each symmetry (7 symmetries in all).

III. Results and Discussion

A. Theoretical Considerations. The orbital energy diagram of 3d orbitals in a pentacoordinate ligand field has been discussed extensively.[23] The reduction in symmetry from O_h to C_{4v} by removal of a CO ligand (Figure 2) stabilizes the e_g orbital oriented along the axis defined by the empty coordination site. In Figure 2 the y axis is chosen as the four-fold axis so that the orbital so designated is d_{y^2}. Much smaller perturbations are anticipated for the t_{2g} orbitals which then transform as e (d_{xy}, d_{yz}) and b_2 (d_{xz}).

Proceeding from the C_{4v} square pyramid (SP) to the D_{3h} trigonal bipyramid (TBP) through the common C_{2v} symmetry, the four lowest d orbitals coalesce into two degenerate pairs e'' (d_{xz}, d_{yz}) and e' $(d_{xy}, d_{x^2-y^2})$ where the z axis now defines the threefold symmetry. From the orbital configuration $(e'')^4(e')^2$ one anticipates a $^3A_2'$ ground state of the TBP. For the SP, depending on the splitting between the (e,b_2) and a_1 orbitals one could imagine a closed-shell $^1A_1$ ground state
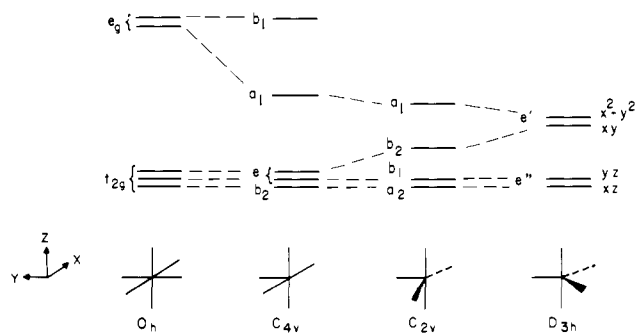
Figure 2. Schematic drawing of the 3d levels in octahedral and various pentacoordinate ligand fields.

Table II. Summary of Valence 3d-Like Orbitals for Selected States of $Cr(CO)_5$ [b]

State	Orbital	n_i	ϵ_i, au [a]	Cr valence population		
				s	p	d
$^1A_1$ (90°)	$3a_2$	2	−0.2339	0.0	0.0	0.69
	$11b_1$	2	−0.2709	0.0	0.0	0.80
	$11b_2$	2	−0.2709	0.0	0.0	0.80
Total (valence orbitals)				0.0	0.0	4.58
Total (all orbitals)				0.38	0.82	5.72
$^3B_2$ (90°	$23a_1$	1	−0.1613	0.09	0.48	0.21
	$3a_2$	2	−0.2989	0.0	0.0	0.76
	$11b_1$	2	−0.3024	0.0	0.0	0.80
	$11b_2$	1	−0.3947	0.0	0.0	0.91
Total (valence orbitals)				0.09	0.48	4.24
Total (all orbitals)				0.45	1.24	5.30
$^3B_2$ (120°)	$23a_1$	1	−0.2375	0.0	0.21	0.53
	$3a_2$	2	−0.3072	0.0	0.0	0.80
	$11b_1$	2	−0.3072	0.0	0.0	0.80
	$11b_2$	1	−0.2389	0.0	0.21	0.54
Total (valence orbitals)				0.0	0.42	4.27
Total (all orbitals)				0.41	1.18	5.39

[a] 1 au = 1 hartree = 27.2117 eV. [b] Mulliken populations for each orbital are normalized to unity.
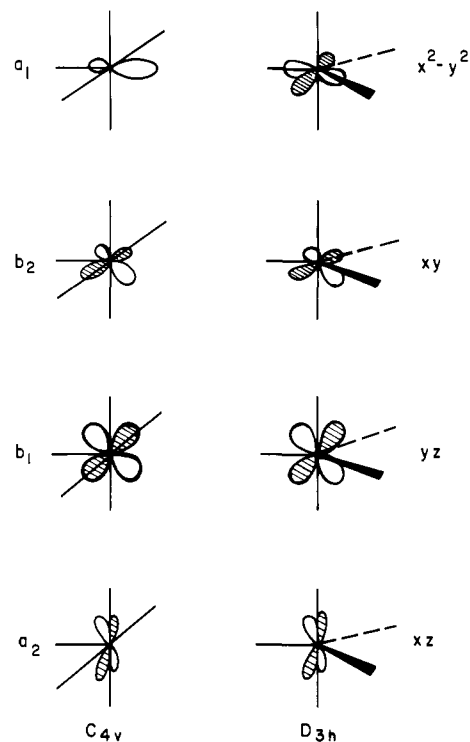

Figure 3. Schematic drawing of the lowest 3d orbitals in $Cr(CO)_5$ for C_{4v} and D_{3h} geometries. Labels refer to C_{2v} symmetry designations.

Table III. Total Charges from Mulliken Population Analysis of Selected States of $Cr(CO)_5$ [a]

State	Cr	$C_{1,2}$	$O_{1,2}$	C_3	O_3	$C_{4,5}$	$O_{4,5}$
$^1A_1$ (90°)	−0.92	+0.35	−0.16	+0.35	−0.17	+0.35	−0.16
$^3B_2$ (90°)	−0.99	+0.32	−0.13	+0.34	−0.12	+0.34	−0.16
$^3B_2$ (120°)	−0.98	+0.33	−0.14	+0.34	−0.15	+0.35	−0.15

[a] Axial ligands are numbered 4 and 5.

$(e)^4(b_2)^2$ analogous to the $(t_{2g})^6$ ground state of $Cr(CO)_6$ or triplet states of $^3E[(e)^3(b_2)^2(a_1)^1]$ or $^3B_2[(e)^4(b_2)^1(a_1)^1]$ symmetry. In the common C_{2v} symmetry the $^3A_2'$ state of the TBP transforms as $^3B_2$ and correlates with one component of the SP ^3E state. The SP $^1A_1$ state ($^1A_1$ in C_{2v}) correlates with one component $^1E'$ of the TBP also arising from the $(e'')^4(e')^2$ configuration.

B. SCF Orbitals and Energies. The shapes of the orbitals from the SCF $^3B_2$ calculations are represented schematically in Figure 3 (where any "back-bonding" to the carbonyls has not been depicted). The a_2, b_1, and b_2 orbitals retain their basic d_{xz}, d_{yz}, and d_{xy} character throughout, but the a_1 orbital undergoes a dramatic change between the SP and TBP. In the SP, instead of resembling d_{y^2} in the earlier idealizations, the orbital is hybridized extensively with 4s and 4p components to protrude into the vacant coordination site. A Mulliken population analysis (Table II) shows the a_1 orbital to be 9% s, 48% p, and 21% d with the remaining amplitude on the carbonyls. (Only qualitative significance should be attached to the precise percentages since the diffuse nature of the 4s, 4p, and $3d''$ components makes the assignment of overlap populations to a particular center quite perilous.) By contrast the other valence orbitals are at least 75% d in character. Bending the CO groups into the TBP restores the $3d^6$ nature of the state (Table II), although the nominally $3d_{xy}$ and $3d_{x^2-y^2}$ orbitals still have substantial p hybridization. The $^1A_1$ state (SP) can be regarded as having a 4s $3d^5$ or 4p $3d^5$ configuration. The total charges on the atoms from the SCF calculations on the $^1A_1$ and $^3B_2$ states are shown in Table III, where the substantial

negative charge on the Cr may be overestimated because of the diffuse basis functions on the metal and the lack of a flexible basis on the CO.

Orbital energies (ϵ_i) from the $^3B_2$ calculations at the various geometries are shown in Figure 4. The $3a_2$ and $11b_1$ orbitals comprising the degenerate e'' pair (d_{xz}, d_{yz}) at $\theta = 120°$ are seen to remain close in energy for all geometries considered. The singly occupied $23a_1$ and $11b_2$ orbitals of the TBP e' pair (d_{xy}, $d_{x^2-y^2}$), on the other hand, are strongly split for other geometries with $\epsilon(b_2) < \epsilon(a_1)$ for $\theta < 120°$ and $\epsilon(a_1) < \epsilon(b_2)$ for $\theta < 120°$. (Although the singly occupied b_2 orbital lies below the doubly occupied orbitals for the SP, this merely reflects the fact that the b_2 and a_1 orbitals are derived from the open-shell Hamiltonian while the remaining orbital orbitals are derived from the closed-shell Hamiltonian. The figure should not be used, therefore in deriving state energies from the sum of orbital energies.)

C. Relative State Energies from SCF and CI Calculations. One of the aims of this study was to ascertain the electronic ground state of $Cr(CO)_5$ and the energy differences between states for various geometric configurations. Since bond lengths were not optimized, any conclusions cannot be considered definitive, but one might hope that the distortions in the pentacarbonyl relative to the hexacarbonyl bond lengths would not be severe.

The relative energies of the prime candidates for the ground state from SCF calculations are presented in Table IV and Figure 5. (We shall refer to all states by their designation in C_{2v} symmetry in the following discussion.) The $^1A_1$ and $^3B_2$
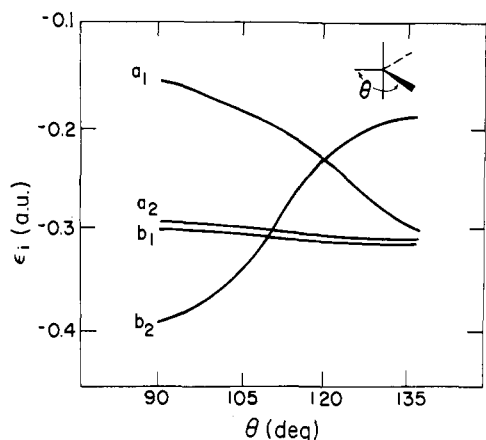
Figure 4. Orbital energies of the 3d orbitals for the $^3B_2$ state of $Cr(CO)_5$ as a function of bending angle.

Table IV. Relative Energies of the States of $Cr(CO)_5$ from SCF and CI Calculations

Geom-etry	State[a]	Config	Total energy, au[b] SCF	Total energy, au[b] CI	Rel energy, kcal/mol SCF	Rel energy, kcal/mol CI
C_{4v}	$^1A_1(^1A_1)$	$(b_2)^2(e)^4$	−0.2318	−0.3740	0	0
C_{4v}	$^3E(^3B_2)$	$(b_2)^2(e)^3$-$(a)^1$	−0.2281	−0.3462	2	9
D_{3h}	$^3A_2'$-$(^3B_2)$	$(e'')^4(e')^2$	−0.2362	−0.3600	−3	17
D_{3h}	$^1E'(^1A_1)$	$(e'')^4(e')^2$		−0.3364		34

[a] C_{2v} designation in parentheses. [b] Relative to −1599.

Table V. Electronic States of $Cr(CO)_5$ for the C_{4v} Geometry

State	C_{2v} designation	Main configuration	Energy, eV
$^1A_1$	$^1A_1$	$(b_2)^2(e)^4(a_1)^0$	0.00
$^1B_2$	$^1A_2$	$(b_2)^1(e)^4(a_1)^1$	1.48
^1E	$^1B_1, ^1B_2$	$(b_2)^2(e)^3(a_1)^2$	1.49 (exptl, 2.0–2.5)
$^1B_2$	$^1A_2$	$(b_2)^2(e)^2(a_1)^2$	3.73
$^1B_1$	$^1A_1$	$(b_2)^1(e)^3(a_1)^2$	4.01
^1E	$^1B_1, ^1B_2$	$(b_2)^2(e)^2(a_1)^2$	4.06
$^1A_1$	$^1A_1$	$(b_2)^2(e)^2(a_1)^2$	4.37
$^1A_1$	$^1A_1$	$(b_2)^0(e)^4(a_1)^2$	5.28
^3E	$^3B_1, ^3B_2$	$(b_2)^2(e)^3(a_1)^1$	0.76
$^3B_2$	$^3A_2$	$(b_2)^1(e)^3(a_1)^2$	1.18
$^3B_2$	$^3A_2$	$(b_2)^2(e)^2(a_1)^2$	2.84
^3E	$^3B_1, ^3B_2$	$(b_2)^2(e)^2(a_1)^2$	3.18

states for the SP ($^1A_1$ and ^3E in C_{4v} notation) lie within a few kcal/mol of each other, and both lie slightly higher than the $^3B_2$ state of the TBP. However, from the considerations discussed earlier one would expect the SCF calculations to have considerable bias toward the states such as the SP $^3B_2$ with a nominal 4s 3d^5 or 4p 3d^5 configuration. In addition, among the 3d^6-like states, one would expect greater electron correlation effects in closed-shell states such as the SP $^1A_1$.

These expectations are borne out by the CI calculations (Figure 5 and Table IV) which place the SP $^1A_1$ state as the ground state with the $^3B_2$ state higher in energy by 17 and 9 kcal/mol in the SP and TBP, respectively. This evidence for a SP $^1A_1$ ground state for $Cr(CO)_5$ is further strengthened by recent SCF calculations on pentacoordinate complexes carried out by Demuynck, Strich, and Veillard.[15] Their basis set, while of roughly comparable accuracy on the metal atom, consisted of a much more flexible [3s 2p] basis on the C and O atoms compared to the minimal [2s 1p] basis employed here. They

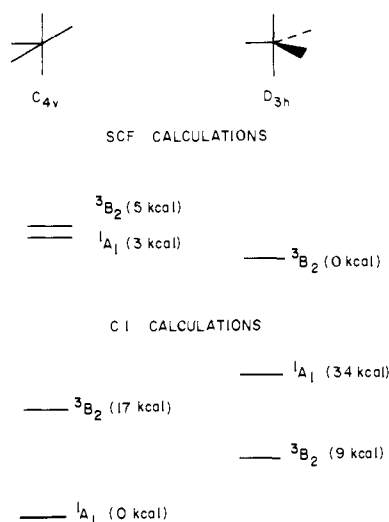**Figure 5.** Lowest electronic states of $Cr(CO)_5$ from SCF and CI calculations.

Table VI. Electronic States of $Cr(CO)_5$ for the D_{3h} Geometry

State	C_{2v} designation	Main configuration	Energy, eV[a]
$^3A_2'$	$^3B_2$	$(e'')^4(e')^2$	0.00
$^3A_1''$	$^3B_1$	$(e'')^3(e')^3$	0.53
$^1E'$	$^1A_1 \ ^1B_2$	$(e'')^4(e')^2$	0.57
$^3A_2''$	$^3A_2$	$(e'')^3(e')^3$	0.74
$^3E''$	$^3A_2, ^3B_1$	$(e'')^3(e')^3$	0.77
$^1A_1'$	$^1A_1$	$(e'')^4(e')^2$	1.17
$^3E''$	$^1A_2, ^1B_1$	$(e'')^3(e')^3$	1.26
$^1A_2''$	$^1A_2$	$(e'')^3(e')^3$	1.35
$^1A_1''$	$^1B_1$	$(e'')^3(e')^3$	1.43
$^3A_2'$	$^3B_2$	$(e'')^2(e')^4$	1.61
$^1E'$	$^1A_1, ^1B_2$	$(e'')^2(e')^4$	2.74
$^1A_1'$	$^1A_1$	$(e'')^2(e')^4$	3.76

[a] Relative to the $^3A_2'$ state, which is calculated to lie 0.38 eV above the ground state at the C_{4v} geometry.

obtain a $^3A_2''$ (TBP)–$^1A_1$ (SP) splitting of 10 kcal/mol compared to −3 kcal/mol here. If the correlation effects are transferable to the larger basis, this would imply a +22 kcal/mol energy splitting ($^3A_2''$ above $^1A_1$) for the two states.

D. Vertical Excitation Energies. The vertical excitation spectrum for the SP and TBP geometries is summarized in Tables V and VI and Figures 6 and 7. All these results have been obtained by the same CI procedure used to obtain the energy differences in the previous section (cf. the section on computational details).

Since the electronic ground state ($^1A_1$) is predicted to have C_{4v} symmetry, we shall concern ourselves first with the excitation spectrum for the SP. The low-lying excited states correspond either to e → a$_1$, or b$_2$ → a$_1$ orbital excitations (Table V) yielding ^1E and ^3E states (1.49 and 0.76 eV) and $^1B_2$ and $^3B_2$ states (1.48 and 1.18 eV), respectively. Of these, only the $^1A_1$ → ^1E transition is dipole allowed. Experimentally, a visible absorption band is observed[7a] in the region 16 000–20 000 cm^{-1} (2.0–2.5 eV) which in all likelihood arises from this transition (calculated at 1.5 eV). A significant transition dipole ($\mu = 1.98$ D), corresponding to an oscillator strength of $f = 0.025$, is calculated for this excitation, which obtains much of its intensity from the 3d → 4p atomic character in the e → a$_1$ transition moment. This agrees well with the observed[1] experimental oscillator strength ($f \sim 0.03$) derived from a molar extinction coefficient (ϵ) 3200. The pronounced variation of the absorption band with the type of solid matrix[5–7] can also
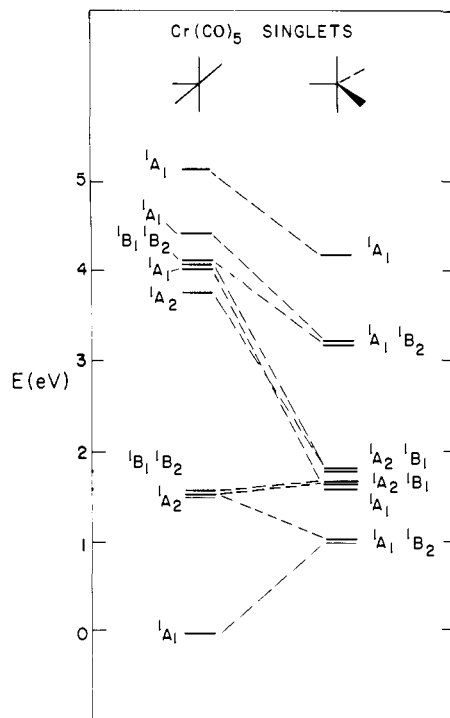
Figure 6. Singlet states of $Cr(CO)_5$ for C_{4v} and D_{3h} geometries as obtained from CI calculations.

Figure 7. Triplet states of $Cr(CO)_5$ for C_{4v} and D_{3h} geometries as obtained from CI calculations.

Figure 8. Electronic states of $Cr(CO)_5$ as a function of equatorial bending angle.

be readily explained on the basis of the spatial extent of the excited state a_1 orbital. This orbital (cf. Figure 3) consists of a (3d, 4s, 4p) lobe extending into the vacant sixth coordination site where it would be expected to interact strongly with any solvent moiety in the vicinity of the first coordination shell. The *destabilization* resulting from the open-shell orbital interaction with the closed-shell solvent will increase in the order Ne < Ar < Kr < Xe in agreement with the shift to higher energies of the $^1A_1 \rightarrow {}^1E$ absorption Ne (16 000 cm⁻¹) < Ar (18 800) < Kr (19 300) < Xe (20 300). Higher electronic states within the 3d manifold correspond to double excitations relative to the $^1A_1$ ground state (Table V) and hence are unlikely to be observed in absorption spectra.

The lowest states of the TBP (Table VI and Figure 6) arise from the configuration $(e'')^4(e')^2$. These include the $^3A_2'$ ground state and $^1E'$ (0.57 eV) and $^1A_1'$ (1.17 eV) excited states. Also in this region are triplet members of the $(e'')^3(e')^3$ manifold—$^3A_1'$ (0.53 eV), $^3A_2''$ and $^3E''$ (0.74–0.77 eV). Since the TBP appears to be the preferred form of the $^3A_2'$ state (see later discussion) the dipole-allowed $^3A_2' \rightarrow {}^3A_2''$ transition (0.74 eV) would be observed if significant numbers of metastable triplet $Cr(CO)_5$ molecules were present in a photochemical process. Recall that the calculations suggest that the TBP triplet lies at least 10 kcal/mol above the singlet SP.

The higher excited states of $Cr(CO)_5$ are expected to be "charge transfer" (metal to ligand) in character, but the present basis set is probably too small to provide a sufficiently accurate description of these states. The lowest virtual orbitals are characterized in Table VII. A dipole-allowed transition is calculated at 4.1 eV arising from 3d → π^* excitations $2b_2 \rightarrow 3b_2$ and $11e \rightarrow 12e$, but more detailed calculations are required before a firm assignment of the 250-nm (5 eV) feature of the $Cr(CO)_5$ absorption spectrum can be made.

E. State Correlations along the SP ↔ TBP Path. The state correlation diagrams for the singlet and triplet states of the SP and TBP are shown in Figures 6 and 7, where C_{2v} symmetry labels are used throughout. The actual calculated curves from the CI results at the other geometries appear in Figure 8 where θ is the OC–Cr–CO equatorial bending angle. Total energies
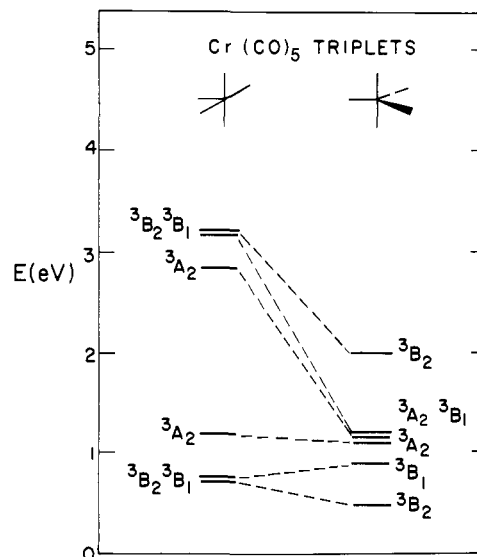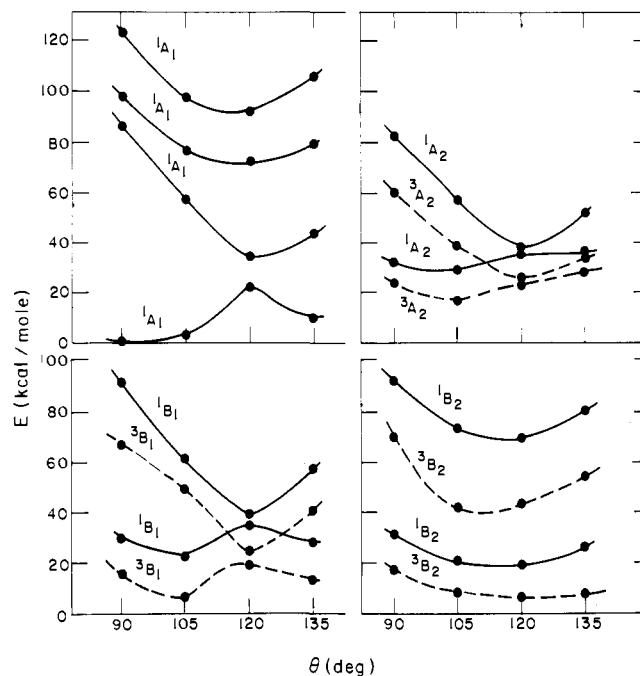
are given in Table VIII. A composite of selected states is depicted in Figure 9. From these curves we may make the following observations.

The $^1A_1$ ground state of the SP increases in energy (~25 kcal/mol) upon bending to become degenerate with a higher state in forming the $^1E'$ state of the TBP. The other member ($^1B_2$) of the $^1E'$ pair corresponds in turn to a member of the ^1E pair of the SP. A Jahn–Teller distortion of the ^1E TBP state therefore stabilizes the $^1A_1$ state and destabilizes the $^1B_2$ state. Between these two states lie three triplet states—the $^3B_2$ with an optimum geometry near the TBP ($^3A_2'$), and the $^3B_1$ and $^3A_2$ states with bond angles near 105°. Another way of viewing the potential energy curve of the $^1A_1$ state is to consider the d orbitals of Figure 3. For $\theta < 120°$ the lowest closed shell singlet state has the configuration $\Phi_1 = (b_1)^2(a_2)^2(b_2)^2$ while for $\theta > 120°$ the lowest $^1A_1$ state is described by the configuration Φ_2

Table VII. Lowest Virtual Orbitals for the SP A_1 State of $Cr(CO)_5{}^b$

Orbital				Population					
C_{2v}	C_{4v}	ϵ_i, au	Type[a]	s_M	p_M	d_M	$CO_{1,2}$	CO_3	$CO_{4,5}$
$23a_1$	$17a_1$	-0.1862	$3d_{y^2}, 4p_y$	0.07	0.40	0.34	0.10	0.03	0.10
$24a_1$	$7b_1$	-0.0661	$3d_{x^2-z^2}$	0.0	0.0	0.90	0.04	0.02	0.12
$25a_1$	$18a_1$	-0.0226	$3d_{y^2}$	0.0	0.05	0.53	0.16	0.14	0.12
$4a_2$	$3b_2$	-0.1329	$3d_{xz}, \pi^*_{CO}$	0.0	0.0	0.65	0.17	0.0	0.17
$12b_1$	$12e$	-0.0925	$3d_{yz}, \pi^*_{CO}$	0.0	0.02	0.51	0.02	0.17	0.28
$13b_1$	$13e$	-0.0460	$4p_z, \pi^*_{CO}$	0.0	0.19	0.03	0.65	0.01	0.12

[a] The y axis represents the fourfold symmetry axis here. [b] The ground state configuration is $(22a_1)^2(3a_2)^2(11b_1)^2(11b_2)^2$ in C_{2v} notation, $(16a_1)^2(2b_2)^2(11e)^4$ in C_{4v}.
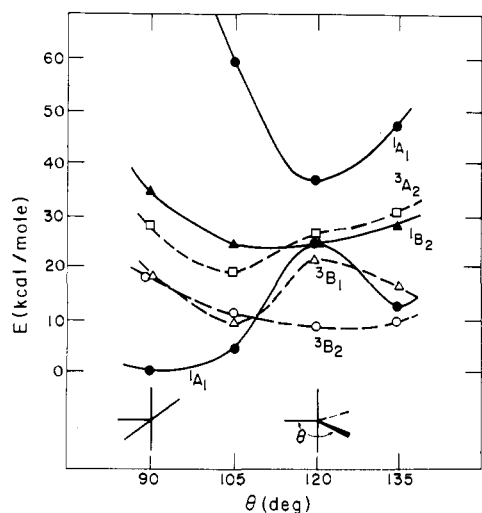
Figure 9. Composite diagram of the lowest electronic states of $Cr(CO)_5$ as a function of equatorial bending angle.

Table VIII. Total Energies (au) as a Function of OC–Cr–CO Equatorial Bond Angle from CI Calculations[c]

State	Root	$\theta = 90°$[a]	$\theta = 90°$[b]	$\theta = 105°$[b]	$\theta = 120°$[b]	$\theta = 135°$[b]
$^1A_1$	1	-0.3740	-0.3703	-0.3683	-0.3364	-0.3540
	2	-0.2263	-0.2320	-0.2789	-0.3169	-0.2989
	3	-0.2135	-0.2137	-0.2488	-0.2544	-0.2443
	4	-0.1800	-0.1736	-0.2126	-0.2218	-0.2022
$^1A_2$	1	-0.3196	-0.3238	-0.3330	-0.3134	-0.3127
	2	-0.2370	-0.2393	-0.2789	-0.3104	-0.2877
$^1B_1$	1	-0.3192	-0.3225	-0.3333	-0.3137	-0.3247
	2	-0.2250	-0.2245	-0.2711	-0.3075	-0.2788
$^1B_2$	1	-0.3194	-0.3205	-0.3362	-0.3392	-0.3284
	2	-0.2248	-0.2247	-0.2546	-0.2594	-0.2433
$^3A_2$	1	-0.3305	-0.3320	-0.3447	-0.3330	-0.3260
	2	-0.2698	-0.2750	-0.3089	-0.3318	-0.3145
$^3B_1$	1	-0.3461	-0.3463	-0.3599	-0.3405	-0.3488
	2	-0.2573	-0.2633	-0.2914	-0.3317	-0.3063
$^3B_2$	1	-0.3462	-0.3426	-0.3569	-0.3600	-0.3591
	2	-0.2572	-0.2585	-0.3037	-0.3007	-0.2847

[a] $^1A_1$ vectors. [b] $^3B_2$ vectors. [c] All energies relative to -1599.

$= (b_1)^2(a_2)^2(a_1)^2$. In general

$$\Phi(1\,^1A_1) = C_1\Phi_1 - C_2\Phi_2$$

$$\Phi(2\,^1A_1) = C_2\Phi_1 + C_1\Phi_2$$

where $C_1 > C_2$ for $\theta < 120°$ and $C_1 < C_2$ for $\theta < 120°$. In the TBP ($\theta = 120°$) the a_1 and b_2 orbitals are degenerate (e') and $C_1 = C_2$. The $1\,^1A_1$ state then has $^1E'$ symmetry while the $2\,^1A_1$ state has $^1A_1'$ symmetry. The maximum of the potential energy curve of the lowest singlet state of $Cr(CO)_5$ can be thus interpreted as resulting from an avoided curve crossing.

F. Photochemical Implications. Although a full geometry optimization for each of the states of $Cr(CO)_5$ was not undertaken, the prediction of a ground state having a SP structure appears to be wholly consistent with the matrix isolation studies. The IR band assignments and ^{13}CO isotopic substitution studies by Turner et al.[7,8] for $Cr(CO)_5$ in matrices—produced either by photolysis of $Cr(CO)_6$ or by cocondensation of Cr atoms with CO—all point to a C_{4v} structure. The cocondensation experiments of Ozin et al.[3,4] yield an interpretation of a D_{3h} structure, but subsequent annealing of the matrix (40–45 K) produces a different form having C_{4v} symmetry.[4] These results have therefore been interpreted[4,7b,9] as evidence for a metastable TBP form which is ultimately converted to the thermodynamically more stable SP form. Since the ground $^3A_2'$ state of the TBP is found to be at least 9 kcal/mol (and possibly as much as 20 kcal/mol or more) higher in energy, the formation of triplet TBP $Cr(CO)_5$ followed by intersystem crossing to the singlet SP ground state is entirely plausible.

Formation of $Cr(CO)_5$ by cocondensation of Cr with CO can be seen to be a likely source of high-spin $Cr(CO)_5$ when one recognizes that the ground state of Cr atom is a ^7S state with extremely high spin multiplicity ($S = 3$) and that the low-lying states are quintet states ($S = 2$). The formation of closed shell $Cr(CO)_6$ by such a route,[7b] however, implies that the obstacles to spin recoupling are not insurmountable.

Interestingly, photodissociation of $Cr(CO)_6$ should yield $Cr(CO)_5$ initially in an excited electronic state since the $^1A_{1g}$ ground state of $Cr(CO)_6$ correlates with the $^1A_1$ ground state of $Cr(CO)_5$.

$$Cr(CO)_6 \rightarrow Cr(CO)_5 + CO$$

The potential energy surface of the electronically excited hexacarbonyl correlates with electronically excited pentacarbonyl.

$$[Cr(CO)_6]^* \rightarrow [Cr(CO)_5]^* + CO$$

Assuming that photodissociation occurs within the singlet manifold, $[Cr(CO)_5]^*$ represents the lowest excited singlet state (^1E for SP, $^1E'$ for TBP). The excited state can eventually yield the $^1A_1$ ground state along certain pathways corresponding to Jahn–Teller distortions interconverting SP and TBP (see Figure 9 and following discussion).

The behavior of the $^1A_1$ and $^1B_2$ states along the bending mode of the equatorial carbonyls suggests a mechanism for photochemical interconversion of axial and equatorial carbonyls (Scheme I). Upon excitation to the ^1E state of the SP, bending either pair of equatorial CO's lowers the energy of the $^1B_2$ component of this state until it becomes degenerate with the $^1A_1$ state at the TBP geometry (Figure 9). The TBP can then continue on the $^1A_1$ state downward along any of three equivalent paths to form SP structures. One of these paths is

Scheme 1
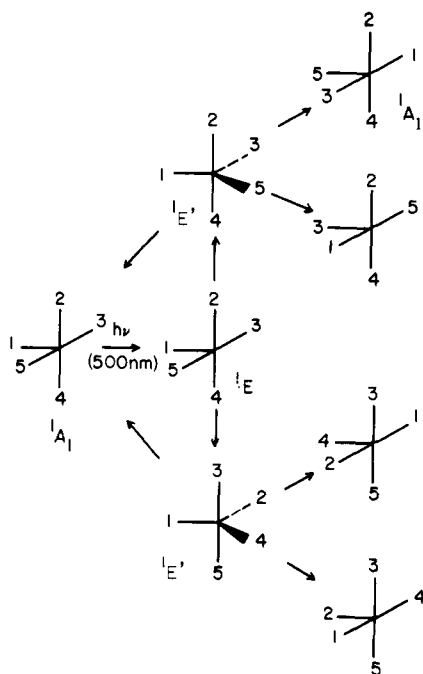
simply the return to the original isomer, but the other paths yield SP structures where the axial groups have been interchanged. The repulsive nature of the ^1E state with a rare gas atom near the sixth site

$$Cr(CO)_5 \cdots S \xrightarrow{h\nu} Cr(CO)_5 \cdots S \rightarrow Cr(CO)_5 + S$$

$$^1A_1 \qquad\qquad ^1E \qquad\qquad ^1E$$
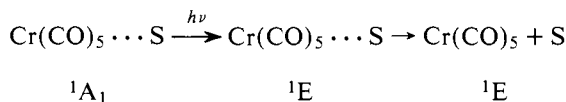
(as discussed earlier in the solvent dependence of the 500-nm absorption band) would facilitate such a rearrangement to a $^1A_1$ state with a different species $Cr(CO)_5 \cdots S'$ near the sixth site. A comprehensive discussion of such rearrangements in matrices (of Ne, Xe, N_2, CO, etc.) as well as a review of other aspects of $Cr(CO)_5$ photochemistry has been given by Turner et al.[24] and by Burdett and Turner.[25]

Another photochemical possibility is metal–metal bond formation. The a_1 lobe orbital of the lowest excited states in Figure 3 is ideally suited for bond formation. The case of $Cr(CO)_5$ is complicated by the presence of a "hole" in the d^6 shell—if we represent the state as $d^5\sigma^1$—whereas $Mn(CO)_5$, represented as $d^6\sigma^1$ in the ground state, readily forms $Mn_2(CO)_{10}$. The apparent nonexistence of $Cr_2(CO)_{10}$ is attributed to (1) the need for forming the dimer from *excited* monomers and (2) the preference for the excited states of the monomer to assume geometries tending toward the TBP which is unfavorable for dimer formation. Neither factor is operable in the case of $Mn(CO)_5$.

IV. Summary

The lowest electronic states of $Cr(CO)_5$ have been investigated using ab initio SCF and CI wave functions in a small Gaussian basis. These calculations represent one of the first studies of electron correlation effects using CI techniques on transition-metal complexes. The ground state is predicted to be the $^1A_1$ state of the SP structure, while the $^3A_2'$ ground state of the TBP is found to lie 9 kcal/mol higher. (A more extensive basis set may lead to a still higher value of $\sim$20 kcal/mol.)

The visible absorption feature at 500 nm is assigned to the $e \rightarrow a_1$ transition of the SP calculated at 1.5 eV (2.0–2.5 eV, experimentally) and an oscillator strength of 0.025 ($f \sim 0.03$, exptl). The extreme dependence of this absorption on the matrix environment can be traced to the lobelike nature of the excited state a_1 orbital which protrudes into the empty sixth coordination site. The electronic states of the pentacarbonyl are examined in terms of the possible roles they may play in its photochemistry.

References and Notes

(1) M. Wrighton, *Chem. Rev.*, **74**, 401 (1974).
(2) A. Vogler in "Concepts in Inorganic Photochemistry", A. W. Adamson and P. D. Fleischauer, Ed., Wiley, New York, N.Y., 1975.
(3) E. P. Kündig and G. A. Ozin, *J. Am. Chem. Soc.*, **96**, 3820 (1974).
(4) H. Huber, E. P. Kündig, G. A. Ozin, and A. J. Poë, *J. Am. Chem. Soc.*, **97**, 308 (1975).
(5) M. A. Graham, M. Poliakoff, and J. J. Turner, *J. Chem. Soc. A*, 2939 (1971).
(6) M. A. Graham, R. N. Perutz, M. Poliakoff, and J. J. Turner, *J. Organomet. Chem.*, **34**, C34 (1972).
(7) (a) R. N. Perutz and J. J. Turner, *J. Am. Chem. Soc.*, **97**, 4791 (1975); (b) *ibid.*, **97**, 4805 (1975).
(8) R. N. Perutz and J. J. Turner, *Inorg. Chem.*, **14**, 262 (1975).
(9) J. D. Black and P. S. Braterman, *J. Am. Chem. Soc.*, **97**, 2908 (1975).
(10) R. V. G. Evans and M. W. Lister, *Trans. Faraday Soc.*, **72**, 1107 (1950).
(11) H. Huber, E. P. Kündig, A. J. Poe, and G. A. Ozin, *J. Am. Chem. Soc.*, **97**, 308 (1975).
(12) L. Hanlan, H. Huber, and G. A. Ozin, *Inorg. Chem.*, **15**, 2592 (1976).
(13) M. Elian and R. Hoffmann, *Inorg. Chem.*, **14**, 1058 (1975).
(14) J. K. Burdett, *J. Chem. Soc., Faraday Trans. 2*, **70**, 1599 (1974); *Inorg. Chem.*, **14**, 375 (1975).
(15) J. Demuynck, A. Strich, and A/ Veillard, *Nouveau J. Chem.*, **1**, 217 (1977).
(16) W. J. Hehre, R. F. Stewart, and J. A. Pople, *J. Chem. Phys.*, **51**, 2657 (1969).
(17) (a) B. Roos, A. Veillard, and G. Vinot, *Theor. Chim. Acta*, **20**, 1 (1971); (b) A. J. H. Wachters, *J. Chem. Phys.*, **52**, 1033 (1970).
(18) R. C. Raffenetti, *J. Chem. Phys.*, **66**, 4377 (1977).
(19) I. H. Hillier and V. R. Saunders, *Mol. Phys.*, **22**, 1025 (1971).
(20) P. J. Hay, *J. Chem. Phys.*, **66**, 4377 (1977).
(21) A. Whitaker and J. W. Jeffery, *Acta Crystallogr.*, **23**, 977 (1967).
(22) W. J. Hunt and W. A. Goddard III, *Chem. Phys. Lett.*, **3**, 414 (1969).
(23) (a) For example, see A. R. Rossi and R. Hoffmann, *Inorg. Chem.*, **14**, 365 (1975), and references in footnote 9. (b) Cf. extensive references in footnote 20 of ref 13.
(24) J. J. Turner, J. K. Burdett, R. H. Perutz, and M. Poliakoff, *Pure Appl. Chem.*, **49**, 271 (1977).
(25) J. K. Burdett and J. J. Turner, *Inorg. Chem.*, in press.
(26) For other examples see B. D. Olafson and W. A. Goddard, *Proc. Natl. Acad. Sci. U.S.A.*, **74**, 1315 (1977).
(27) S. P. Walch and W. A. Goddard III, *J. Am. Chem. Soc.*, **98**, 7908 (1976).